UDC 519.61:531.3:624.07
Original scientific paper
Received: 25.08.2014.

Vibrations of fixed-fixed heterogeneous curved beams loaded by a central force at the crown point

László Kiss[(1)], **György Szeidl**[(1)], **Sorin Vlase**[(2)], **Botond Pál Gálfi**[(2)], **Péter Dani**[(2)], **Ildikó Renata Munteanu**[(2)], **Raluca Dora Ionescu**[(2)] and **János Száva**[(2)]

[(1)]Institute of Applied Mechanics, University of Miskolc, 3515 Miskolc-Egyetemváros, HUNGARY
e-mail: mechkiss@uni-miskolc.hu, gyorgy.szeidl@uni-miskolc.hu
[(2)]Department of Mechanical Engineereing, Transilvania University of Brasov, Brasov, ROMANIA

SUMMARY

This paper addresses the vibrations of heterogeneous curved beams under the assumption that the load of the beam is a dead one and is perpendicular to the centroidal axis. It is assumed that: (a) the radius of curvature is constant, and (b) Young's modulus and the Poisson's number depend on the cross-sectional coordinates. As for the issue of fixed-fixed beams, the objectives are the following: (1) to determine the Green's function matrices provided that the beam is under radial load; (2) to examine how the load affects the natural frequencies given that the beam is subjected to a vertical force at the crown point; (3) to develop a numerical model which makes it possible to determine how the natural frequencies are related to the load. The computational results are presented graphically.

Key words: *curved beams, heterogeneous material, natural frequency as a function of the load, Green's function matrices.*

1. INTRODUCTION

Curved beams are used in various engineering applications. Arch bridges, roof structures and stiffeners in aerospace applications are some of them. Research into the mechanical behaviour of curved beams began in the 19th century – see book [1] by Love for further details. The free vibrations of curved beams have also been extensively investigated. Three survey papers are worth mentioning: Refs. [2], [3] and [4]. A Ph.D. Thesis [5] is also worth mentioning in this context. The thesis clarifies, within the frames of the linear theory, how the extensibility of the centerline affects the free vibrations and stability of circular beams subjected to constant radial load (a dead load). Solutions to the natural frequencies were computed utilizing different numerical models. One of these is based on the use of the Green's function matrix that belongs to the corresponding boundary value problem. Unfortunately, the results of Ref. [5] have not been published in English. Paper [6] takes shear deformations into account provided that the beam vibrates under the action of a constant vertical distributed load.

Free vibrations of spatial curved beams made of functionally graded material are presented in Ref. [7], while laminated curved beams are investigated in Ref. [8]. Paper [9] by Kovacs deals with the vibrations of layered arches assuming perfect or imperfect bonding between any two adjacent layers. Forced vibrations of curved beams on elastic foundation are considered in Ref. [10].

Lawther addresses the problem of how a prestressed state of the body affects the natural frequencies [11]. He studies finite dimensional multiparameter eigenvalue problems and comes to the conclusion that, for such problems, the eigenvalue part of the solution is described by interaction curves in an eigenvalue space, and every such eigenvalue solution has an associated eigenvector. If all points on a curve have the same eigenvector, then the curve is necessarily

a straight line, but the converse situation is far more complex.

In the light of these results, a question arises: how do natural frequencies change if a curved beam is subjected to radial (vertical) load at the crown point. In our research, it is assumed that the curved beam is made of heterogeneous, isotropic and linearly elastic material. As regards heterogeneity, it is assumed that the elastic parameters can be varied arbitrarily over the beam's cross-section but they are independent of the coordinate perpendicular to the cross-section. Under these assumptions our main objectives are as follows: (1) derivation of boundary value problems which make it possible to understand how the radial load affects the natural frequencies; (2) determination of the Green's function matrices which can be used to reduce the eigenvalue problem set up for the natural frequencies (which depend on the load) to an eigenvalue problem governed by systems of Fredholm integral equations; (3) to reduce the eigenvalue problem to an algebraic one i.e. to a one that can be solved numerically. The corresponding computational results are presented in a graphical format and are verified against the experimental results.

The paper is organized in eight sections. Section 2 is a summary of the governing equations. In Section 3, having defined the Green's function matrices, we reduced the eigenvalue problem to an eigenvalue problem governed by Fredholm integral equations. Section 4 gives an outline of the solution algorithm. Calculation of the Green's function matrices are detailed in Section 5. Relationship between the axial strain on the centroidal axis and the load are presented in Section 6, which also contains a formula for the critical value of the strain. Computational and experimental results are shown in Section 7. Conclusions are presented in Section 8.

2. BASIC ASSUMPTIONS AND GOVERNING RELATIONS

2.1 Equations valid for distributed load

Based on article [12], the governing formulae of the dynamical problem are presented hereinafter. In Figure 1(a) a part of the beam is illustrated with the applied curvilinear coordinate system ($\xi = s,\eta,\zeta$) and Figure 1(b) shows the investigated fixed-fixed beam. The cross-section of the beam is uniform and symmetric with respect to the axis ζ. The material parameters, such as Young's modulus, E, and the Poisson number, ν, can depend on the cross-sectional coordinates in such a way that: $E(\eta,\zeta) = E(-\eta,\zeta)$; $\nu(\eta,\zeta) = \nu(-\eta,\zeta)$.

Notice that the coordinate line $\xi = s$ coincides with the so-called E - weighted centroidal axis (or centroidal axis for short). This axis intersects the cross-section at the point C and its position can be obtained from the condition:

$$Q_{e\eta} = \int_A E(\eta,\zeta)\,\zeta\,dA = 0\,, \tag{1}$$

which means that the E - weighted first moment of the cross section with respect to the axis η vanishes there.

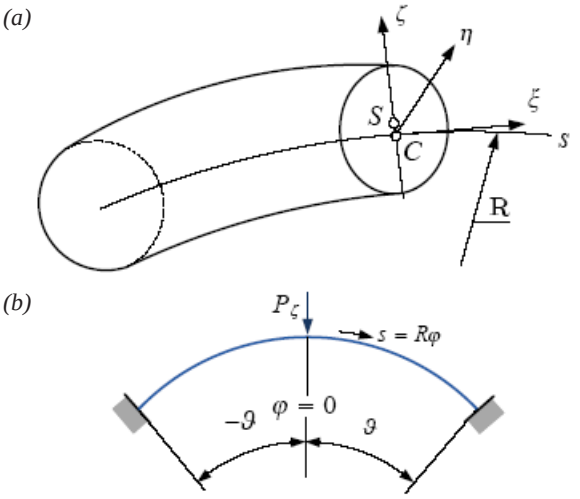

Fig. 1 (a) The coordinate system; (b) Fixed-fixed beam under concentrated load

For our further considerations we shall introduce the the quantities A_e and $I_{e\eta}$ defined by equations:

$$A_e = \int_A E(\eta,\zeta)\,dA\,, \quad I_{e\eta} = \int_A E(\eta,\zeta)\,\zeta^2\,dA\,. \tag{2}$$

These are referred to as the E - weighted area and the E - weighted moment of inertia, respectively.

Subsequently, we separate the load-induced, and otherwise time-independent quantities from those in relation with the vibrations of the loaded beam. The latter are the time-dependent increments and are denoted by a subscript $_b$. Let u_o, w_o and R be the tangential and radial displacements and the constant radius of the centroidal axis. The relation between the coordinate line s and the angle coordinate φ is $s=R\varphi$.

The axial strain $\varepsilon_{o\xi}$ and the rotation $\psi_{o\eta}$ on the centroidal axis can be expressed in terms of the displacements via relations:

$$\varepsilon_{o\xi} = \frac{du_o}{ds} + \frac{w_o}{R}\,, \quad \psi_{o\eta} = \frac{u_o}{R} - \frac{dw_o}{ds}\,. \tag{3}$$

Application of the principle of virtual work (details are omitted) yields that the axial force N and the bending moment M should satisfy equilibrium equations:

$$\frac{dN}{ds} + \frac{1}{R}\left[\frac{dM}{ds} - \left(N + \frac{M}{R}\right)\psi_{o\eta}\right] + f_t = 0\,, \tag{4a}$$

$$\frac{d}{ds}\left[\frac{dM}{ds} - \left(N + \frac{M}{R}\right)\psi_{o\eta}\right] - \frac{N}{R} + f_n = 0\,, \tag{4b}$$

where f_t and f_n are the intensity of the distributed load in the tangential and normal directions. The Hooke's

law yields the connection between the inner forces and the displacements [12]:

$$N = A_e\varepsilon_{o\xi} - \frac{M}{R}, \qquad M = -I_{e\eta}\left(\frac{d^2 w_o}{ds^2} + \frac{w_o}{R^2}\right), \tag{5}$$

$$N + \frac{M}{R} = \frac{I_{e\eta}}{R^2}\varepsilon_{o\xi}\,. \tag{6}$$

Let us now introduce the dimensionless displacements and a consistent notation for the derivatives:

$$U_o = \frac{u_o}{R}, \quad W_o = \frac{w_o}{R}; \qquad (\ldots)^{(n)} = \frac{d^n(\ldots)}{d\varphi^n}, \quad n = 1,2,\ldots\,. \tag{7}$$

Substituting Hooke's law, Eq. (5), and, after that, the kinematical quantities, Eq. (3), into equilibrium Eqs. (4), we get the system of differential equations:

$$\begin{bmatrix} 0 & 0 \\ 0 & 1 \end{bmatrix}\begin{bmatrix} U_o \\ W_o \end{bmatrix}^{(4)} + \begin{bmatrix} -m & 0 \\ 0 & 2 - m\varepsilon_{o\xi} \end{bmatrix}\begin{bmatrix} U_o \\ W_o \end{bmatrix}^{(2)} + \begin{bmatrix} 0 & -m \\ m & 0 \end{bmatrix}\begin{bmatrix} U_o \\ W_o \end{bmatrix}^{(1)} + \begin{bmatrix} 0 & 0 \\ 0 & 1 + m\left(1 - \varepsilon_{o\xi}\right) \end{bmatrix}\begin{bmatrix} U_o \\ W_o \end{bmatrix} = \frac{R^3}{I_{e\eta}}\begin{bmatrix} f_t \\ f_n \end{bmatrix}, \quad \text{where} \quad m = \frac{A_e R^2}{I_{e\eta}} - 1\,. \tag{8}$$

Assume now that the strain has a negligible effect on the equilibrium, i.e. $\varepsilon_{o\xi} = 0$. In this respect, the previous equation simplifies into the form:

$$\begin{bmatrix} 0 & 0 \\ 0 & 1 \end{bmatrix}\begin{bmatrix} U_o \\ W_o \end{bmatrix}^{(4)} + \begin{bmatrix} -m & 0 \\ 0 & 2 \end{bmatrix}\begin{bmatrix} U_o \\ W_o \end{bmatrix}^{(2)} + \begin{bmatrix} 0 & -m \\ m & 0 \end{bmatrix}\begin{bmatrix} U_o \\ W_o \end{bmatrix}^{(1)} + \begin{bmatrix} 0 & 0 \\ 0 & 1 + m \end{bmatrix}\begin{bmatrix} U_o \\ W_o \end{bmatrix} = \frac{R^3}{I_{e\eta}}\begin{bmatrix} f_t \\ f_n \end{bmatrix}. \tag{9}$$

2.2 Governing equations for the increments

It can be demonstrated that the increment in the axial strain and in the rotation field have a similar structure to Eqs. (3):

$$\varepsilon_{mb} = \varepsilon_{o\xi b} + \psi_{o\eta}\psi_{o\eta b}, \quad \psi_{o\eta b} = \frac{u_{ob}}{R} - \frac{\partial w_{ob}}{\partial s} \tag{10}$$

$$\varepsilon_{o\xi b} = \frac{\partial u_{ob}}{\partial s} + \frac{w_{ob}}{R}\,. \tag{11}$$

It can, in addition, be verified that the differential equations the increments in the inner forces should satisfy are of the following forms:

$$\frac{\partial}{\partial s}\left(N_b + \frac{M_b}{R}\right) - \frac{1}{R}\left(N + \frac{M}{R}\right)\psi_{o\eta b} + f_{tb} = 0\,, \tag{12a}$$

and:

$$\frac{\partial^2 M_b}{\partial s^2} - \frac{N_b}{R} - \frac{\partial}{\partial s}\left[\left(N + \frac{M}{R}\right)\psi_{o\eta b} + \left(N_b + \frac{M_b}{R}\right)\psi_{o\eta}\right] + f_{nb} = 0\,. \tag{12b}$$

Since the investigated process is dynamical – and in this case there is no change in the initial load – it follows that the increments f_{tb} and f_{nb} are actually forces of inertia, therefore:

$$f_{tb} = -\rho_a A\frac{\partial^2 u_{ob}}{\partial t^2}, \quad f_{nb} = -\rho_a A\frac{\partial^2 w_{ob}}{\partial t^2}\,. \tag{13}$$

Here A is the area of the cross-section and ρ_a is the average density over the cross-section. Based on the aforementioned, recalling Hooke's law, we obtain:

$$N_b = \frac{I_{e\eta}}{R^2}m\varepsilon_{o\xi b} - \frac{M_b}{R}, \qquad M_b = -I_{e\eta}\left(\frac{\partial^2 w_{ob}}{\partial s^2} + \frac{w_{ob}}{R^2}\right), \qquad N_b + \frac{M_b}{R} = \frac{I_{e\eta}}{R^2}m\varepsilon_{o\xi b}\,. \tag{14}$$

A comparison of Eqs. (10), (12) and (14) results in the equations of motion:

$$\begin{bmatrix} 0 & 0 \\ 0 & 1 \end{bmatrix}\begin{bmatrix} U_{ob} \\ W_{ob} \end{bmatrix}^{(4)} + \begin{bmatrix} -m & 0 \\ 0 & 2 - m\varepsilon_{o\xi} \end{bmatrix}\begin{bmatrix} U_{ob} \\ W_{ob} \end{bmatrix}^{(2)} + \begin{bmatrix} 0 & -m \\ m & 0 \end{bmatrix}\begin{bmatrix} U_{ob} \\ W_{ob} \end{bmatrix}^{(1)} + \begin{bmatrix} 0 & 0 \\ 0 & 1 + m\left(1 - \varepsilon_{o\xi}\right) \end{bmatrix}\begin{bmatrix} U_{ob} \\ W_{ob} \end{bmatrix} = \frac{R^3}{I_{e\eta}}\begin{bmatrix} f_{tb} \\ f_{nb} \end{bmatrix}. \tag{15}$$

Observe that we have linearized the problem: (a) we neglected the quadratic term $\varepsilon_{o\xi}\,\varepsilon_{o\xi\,b}$ in (12a); (b) we considered the validity of the inequalities $\varepsilon_{o\xi\,b} >> (\varepsilon_{o\xi b}\psi_{o\eta})^{(1)}$ and $1 >> \varepsilon_{o\xi}$ in (12b) when utilizing Hooke's law.

If we assume harmonic vibrations and denote the dimensionless displacement amplitudes by $\hat{U}_{ob}$ and $\hat{W}_{ob}$ then we have:

$$\begin{bmatrix}0 & 0\\ 0 & 1\end{bmatrix}\begin{bmatrix}\hat{U}_{ob}\\ \hat{W}_{ob}\end{bmatrix}^{(4)}+\begin{bmatrix}-m & 0\\ 0 & 2-m\varepsilon_{o\xi}\end{bmatrix}\begin{bmatrix}\hat{U}_{ob}\\ \hat{W}_{ob}\end{bmatrix}^{(2)}+$$
$$+\begin{bmatrix}0 & -m\\ m & 0\end{bmatrix}\begin{bmatrix}\hat{U}_{ob}\\ \hat{W}_{ob}\end{bmatrix}^{(1)}+\begin{bmatrix}0 & 0\\ 0 & 1+m\left(1-\varepsilon_{o\xi}\right)\end{bmatrix}\begin{bmatrix}\hat{U}_{ob}\\ \hat{W}_{ob}\end{bmatrix}=$$
$$=\lambda\begin{bmatrix}\hat{U}_{ob}\\ \hat{W}_{ob}\end{bmatrix};\qquad \lambda=\rho_a A\frac{R^3}{I_{e\eta}}\alpha^2. \tag{16}$$

Here λ and α are the eigenvalue and sought natural frequency.

For an unloaded beam, i.e. when $\varepsilon_{o\xi}=0$ – we obtain the equations which govern the free vibrations; compare equation:

$$\begin{bmatrix}0 & 0\\ 0 & 1\end{bmatrix}\begin{bmatrix}\hat{U}_{ob}\\ \hat{W}_{ob}\end{bmatrix}^{(4)}+\begin{bmatrix}-m & 0\\ 0 & 2\end{bmatrix}\begin{bmatrix}\hat{U}_{ob}\\ \hat{W}_{ob}\end{bmatrix}^{(2)}+$$
$$+\begin{bmatrix}0 & -m\\ m & 0\end{bmatrix}\begin{bmatrix}\hat{U}_{ob}\\ \hat{W}_{ob}\end{bmatrix}^{(1)}+\begin{bmatrix}0 & 0\\ 0 & m+1\end{bmatrix}\begin{bmatrix}\hat{U}_{ob}\\ \hat{W}_{ob}\end{bmatrix}=\lambda\begin{bmatrix}\hat{U}_{ob}\\ \hat{W}_{ob}\end{bmatrix} \tag{17}$$

to Eq. (11) in Ref. [13]. Depending on the supports, the above system is associated with appropriate boundary conditions. Note that the left side of Eq. (16) – or that of Eq. (15) – can be rewritten in the form:

$$\mathbf{K}\left[\mathbf{y}(\varphi),\varepsilon_{o\xi}\right]=\overset{4}{\mathbf{P}}\mathbf{y}^{(4)}+\overset{2}{\mathbf{P}}\mathbf{y}^{(2)}+\overset{1}{\mathbf{P}}\mathbf{y}^{(1)}+\overset{0}{\mathbf{P}}\mathbf{y}^{(0)},$$
$$\mathbf{y}=\begin{bmatrix}\hat{U}_{ob}\\ \hat{W}_{ob}\end{bmatrix}. \tag{18}$$

Ordinary differential equations (ODEs), Eqs. (17), (or which is the same, Eqs. (18)) and the corresponding homogeneous boundary conditions together constitute eigenvalue problems.

Observe that the i-th eigenfrequency α_i in these eigenvalue problems depends on the magnitude of the concentrated force P_ζ, or what is the same, on the dimensionless load $\mathcal{P}=P_\zeta R^2\vartheta/(2I_{e\eta})$ through the axial strain: $\varepsilon_{o\xi}=\varepsilon_{o\xi}(\mathcal{P})$. Also note that heterogeneity in the material appears in the formulation via the parameters m and ρ_a.

3. GREEN'S FUNCTION MATRIX

Differential equations (18) is degenerated as the matrix:

$$\overset{4}{\boldsymbol{P}}=\begin{bmatrix}0 & 0\\ 0 & 1\end{bmatrix} \tag{19}$$

has no inverse. Let $\boldsymbol{r}(\varphi)$ be a prescribed inhomogeneity. Consider the boundary value problem defined by the ordinary differential equations:

$$\mathbf{K}(\mathbf{y})=\sum_{\nu=0}^{4}\overset{\nu}{\mathbf{P}}(\varphi)\mathbf{y}^{(\nu)}(\varphi)=\mathbf{r}(\varphi),$$
$$\overset{3}{\mathbf{P}}(\varphi)=\mathbf{0} \tag{20a}$$

and the homogeneous boundary conditions valid for fixed-fixed beams (the displacements and the rotations are zero at the ends):

$$\hat{U}_{ob}\big|_{\pm\vartheta}=\hat{W}_{ob}\big|_{\pm\vartheta}=\hat{W}_{ob}^{(1)}\big|_{\pm\vartheta}=0. \tag{20b}$$

Solution to the homogeneous part of equations (20a) depends on whether the axial strain $\varepsilon_{o\xi}$ is positive or negative. Let:

$$\chi^2=\begin{cases}1-m\varepsilon_{o\xi} & \text{if} \quad m\varepsilon_{o\xi}<1\\ m\varepsilon_{o\xi}-1 & \quad\quad m\varepsilon_{o\xi}>1.\end{cases} \tag{21}$$

If $m\varepsilon_{o\xi}<1$, solution to the homogeneous part assumes the form:

$$\mathbf{y}=\left[\sum_{i=1}^{4}\underset{(2\times2)}{\mathbf{Y}}{}_i\,\underset{(2\times2)}{\mathbf{C}}{}_i\right]\underset{(2\times1)}{\mathbf{e}}, \tag{22a}$$

where:

$$\mathbf{Y}_1=\begin{bmatrix}\cos\varphi & 0\\ \sin\varphi & 0\end{bmatrix},\quad \mathbf{Y}_2=\begin{bmatrix}-\sin\varphi & 0\\ \cos\varphi & 0\end{bmatrix},$$
$$\mathbf{Y}_3=\begin{bmatrix}\cos\chi\varphi & \mathcal{M}\varphi\\ \chi\sin\chi\varphi & -1\end{bmatrix},\quad \mathbf{Y}_4=\begin{bmatrix}-\sin\chi\varphi & 1\\ \chi\cos\chi\varphi & 0\end{bmatrix}. \tag{22b}$$

It can be verified that if $m\varepsilon_{o\xi}>1$, $\mathbf{Y}_3$ and $\mathbf{Y}_4$ change into:

$$\mathbf{Y}_3=\begin{bmatrix}\cosh\chi\varphi & \mathcal{M}\varphi\\ \chi\sinh\chi\varphi & -1\end{bmatrix},\quad \mathbf{Y}_4=\begin{bmatrix}-\sinh\chi\varphi & 1\\ \chi\cosh\chi\varphi & 0\end{bmatrix}. \tag{22c}$$

In the above equations, $\mathbf{C}_i$ are arbitrary constant matrices, $\mathbf{e}$ is an arbitrary column matrix and:

$$\mathcal{M}=\frac{m+1}{m\left(1+\varepsilon_{o\xi}\right)}. \tag{22d}$$

Solution to the boundary value problem governed by (20a) and (20b) is sought in the form:

$$\mathbf{y}(\varphi)=\int_{-\vartheta}^{\vartheta}\mathbf{G}(\varphi,\psi)\mathbf{r}(\psi)d\psi,$$
$$\mathbf{G}(\varphi,\psi)=\begin{bmatrix}G_{11}(\varphi,\psi) & G_{12}(\varphi,\psi)\\ G_{21}(\varphi,\psi) & G_{22}(\varphi,\psi)\end{bmatrix}, \tag{23}$$

where $\mathbf{G}(\varphi,\psi)$ is Green's function matrix defined by the following properties [5]:

1) The Green's function matrix is a continuous function of φ and ψ in each of the triangles $-\vartheta\le\varphi\le\psi\le\vartheta$ and $-\vartheta\le\psi\le\varphi\le\vartheta$. The functions ($G_{11}(\varphi,\psi)$, $G_{12}(\varphi,\psi)$) [$G_{21}(\varphi,\psi)$, $G_{22}(\varphi,\psi)$] are (2 times) [4 times] differentiable with respect to φ, and the derivatives:

$$\frac{\partial^{\nu}\mathbf{G}(\varphi,\psi)}{\partial\varphi^{\nu}}=\mathbf{G}^{(\nu)}(\varphi,\psi)\quad(\nu=1,2),$$

$$\frac{\partial^{\nu}G_{2i}(\varphi,\psi)}{\partial\varphi^{\nu}}=G_{2i}^{(\nu)}(\varphi,\psi)\quad(\nu=1,2,3,4;\,i=1,2) \tag{24}$$

are continuous functions of φ and ψ.

2) Let ψ be fixed in $[-\vartheta,\vartheta]$. Although the function and the derivatives:

$$\begin{aligned}&G_{11}(\varphi,\psi),\quad G_{12}^{(1)}(\varphi,\psi),\\&G_{21}^{(\nu)}(\varphi,\psi)\ (\nu=1,2,3),\\&G_{22}^{(\nu)}(\varphi,\psi)\ (\nu=1,2)\end{aligned} \tag{25a}$$

are continuous everywhere, the derivatives $G_{11}^{(1)}(\varphi,\psi)$ and $G_{22}^{(3)}(\varphi,\psi)$ have a jump at $\varphi=\psi$:

$$\lim_{\varepsilon\to 0}\left[G_{11}^{(1)}(\varphi+\varepsilon,\varphi)-G_{11}^{(1)}(\varphi-\varepsilon,\varphi)\right]=1/\overset{2}{P}_{11}(\varphi), \tag{25b}$$

$$\lim_{\varepsilon\to 0}\left[G_{22}^{(3)}(\varphi+\varepsilon,\varphi)-G_{22}^{(3)}(\varphi-\varepsilon,\varphi)\right]=1/\overset{4}{P}_{22}(\varphi). \tag{25c}$$

3) Let $\boldsymbol{\alpha}$ be an arbitrary, otherwise constant vector. For a fixed $\psi\in[-\vartheta,\vartheta]$, the vector $\mathbf{G}(\varphi,\psi)\,\boldsymbol{\alpha}$, as a function of $\varphi(\varphi\neq\psi)$, should satisfy the homogeneous differential equations $\mathbf{K}\,[\,\mathbf{G}(\phi,\psi)\,\boldsymbol{\alpha}\,]=\mathbf{0}$.
4) The vector $\mathbf{G}(\varphi,\psi)\,\boldsymbol{\alpha}$, as a function of φ, should satisfy the boundary conditions in Eq. (20b). In addition, a one, unique Green's function matrix belongs to the boundary value problem considered here.

If Green's function matrix exists, then vector (3) satisfies differential equation (20a) and boundary conditions (20b).

Consider now differential equations of the form:

$$\mathbf{K}[\mathbf{y}]=\lambda\,\mathbf{y} \tag{26}$$

where $\mathbf{K}[\mathbf{y}]$ is given by Eq. (18) and λ is a parameter (the eigenvalue sought). The system of ordinary differential equations (26) is associated with homogeneous boundary conditions (20b) to constitute a boundary value problem.

The vectors $\mathbf{u}^T=[u_1\,|\,u_2]$ and $\mathbf{v}^T=[v_1\,|\,v_2]$ are comparison vectors, if they are different from zero, satisfy the boundary conditions and are differentiable as many times as required.

The eigenvalue problem given by Eqs. (26) and (20b) is self-adjoint if the product $(\mathbf{u},\mathbf{v})_M=\int_{-\vartheta}^{\vartheta}\mathbf{u}^T\mathbf{K}\mathbf{v}\,d\varphi$ is commutative, i.e. $(\mathbf{u},\mathbf{v})_M=(\mathbf{v},\mathbf{u})_M$ over the set of comparison vectors and it is positive definite if $(\mathbf{u},\mathbf{u})_M>0$ for any comparison vector $\mathbf{u}$.

If the eigenvalue problem given by Eqs. (26) and (20b) is self-adjoint, then Green's function matrix is cross-symmetric: $\boldsymbol{G}(\varphi,\psi)=\boldsymbol{G}^{\boldsymbol{T}}(\psi,\varphi)$.

4. NUMERICAL SOLUTION TO THE EIGENVALUE PROBLEMS

Employing Eq. (3), the eigenvalue problem given by Eqs. (26) and (20b) can be replaced by a homogeneous integral equation system, which has the following form:

$$\mathbf{y}(\varphi)=\lambda\int_{-\vartheta}^{\vartheta}\mathbf{G}(\varphi,\psi)\mathbf{y}(\psi)d\psi\,. \tag{27}$$

Numerical solution to the eigenvalue problem determined by Eq. (27) can be sought by quadrature methods [14]. Consider the integral formula:

$$\begin{aligned}&J(\phi)=\int_{-\vartheta}^{\vartheta}\phi(\psi)d\psi\equiv\sum_{j=0}^{n}w_j\phi(\psi_j)\\&\psi_j\in[-\vartheta,\vartheta],\end{aligned} \tag{28}$$

where $\psi_j(\varphi)$ is a vector and the weights w_j are known. Having utilized the latter equation, we obtain from Eq. (27) that:

$$\begin{aligned}&\sum_{j=0}^{n}w_j\mathbf{G}(\varphi,\psi_j)\tilde{\mathbf{y}}(\psi_j)=\tilde{\kappa}\tilde{\mathbf{y}}(\varphi),\\&\tilde{\kappa}=1/\tilde{\lambda}\qquad\psi_j\in[-\vartheta,\vartheta]\end{aligned} \tag{29}$$

is the solution, which yields an approximate eigenvalue $\tilde{\lambda}=1/\tilde{\kappa}$ and a corresponding approximate eigenfunction $\tilde{\mathbf{y}}(\varphi)$. After setting φ to $\psi_i(i=0,1,2,...,n)$ we have:

$$\begin{aligned}&\sum_{j=0}^{n}w_j\mathbf{G}(\psi_i,\psi_j)\tilde{\mathbf{y}}(\psi_j)=\tilde{\kappa}\tilde{\mathbf{y}}(\psi_i)\\&\tilde{\kappa}=1/\tilde{\lambda}\qquad\psi_i,\psi_j\in[-\vartheta,\vartheta]\end{aligned} \tag{30}$$

or:

$$\mathcal{G}\mathcal{D}\tilde{\mathcal{Y}}=\tilde{\kappa}\tilde{\mathcal{Y}}\,, \tag{31}$$

where $\mathcal{G}=[\mathbf{G}(\psi_i,\psi_j)]$ is symmetric when the problem is self-adjoint. Moreover:

$$\mathcal{D}=diag(\underbrace{w_0,...,w_0}_{n=2}\,|\,...\,|\,\underbrace{w_n,...,w_n}_{n=2})$$

and $\tilde{\mathcal{Y}}^T=[\mathbf{y}^T(\psi_0)\,|\,\tilde{\mathbf{y}}^T(\psi_1)\,|\,...\,|\,\tilde{\mathbf{y}}^T(\psi_n)]$. After solving the generalized algebraic eigenvalue problem (31) we have the approximate eigenvalues $\tilde{\lambda}_r$ and eigenvectors $\tilde{\mathcal{Y}}_r$, while the corresponding eigenfunction is obtained by a substitution into Eq. (29), so that:

$$\begin{aligned}&\tilde{\mathbf{y}}_r(\varphi)=\tilde{\lambda}_r\sum_{j=0}^{n}w_j\mathbf{G}(\varphi,\psi_j)\tilde{\mathbf{y}}_r(\psi_j)\\&r=0,1,2,\ldots,n\,.\end{aligned} \tag{32}$$

Divide the range $[-\vartheta,\vartheta]$ into equidistant subintervals of length h and apply the integration

formula to each subinterval. By repeating the line of thought leading to Eq. (32), one can show that the algebraic eigenvalue problem obtained has the same structure as Eq. (32).

It is also possible to consider the integral equation (27) as if it were a boundary integral equation and apply isoparametric approximation on the subintervals, i.e. on the elements. If this is the case, one can approximate the eigenfunction on the *e*-th element (the *e*-th subinterval, which is mapped onto the interval $\gamma \in [-1,1]$ and is denoted by $\mathfrak{L}_e$) by:

$$\overset{e}{\mathbf{y}} = \mathbf{N}_1(\gamma)\overset{e}{\mathbf{y}}_1 + \mathbf{N}_2(\gamma)\overset{e}{\mathbf{y}}_2 + \mathbf{N}_3(\gamma)\overset{e}{\mathbf{y}}_3 , \quad (33)$$

where quadratic local approximation is utilized with $\mathbf{N}_i = diag(N_i)$, $N_1 = 0.5\ \gamma\ (\gamma-1)$, $N_2 = 1-\gamma^2$, $N_3 = 0.5\ \gamma(\gamma+1)$, $\mathbf{y}_i$ is the value of the eigenfunction $\mathbf{y}(\varphi)$ at the left endpoint, the midpoint and the right endpoint of the element, respectively. Upon the substitution of approximation given by Eq. (33) into Eq. (27) we have:

$$\tilde{\mathbf{y}}(\varphi) = \tilde{\lambda}\sum_{e=1}^{n_{be}}\int_{\mathfrak{L}_e}\mathbf{G}(\varphi,\gamma)\mathbf{N}(\gamma)d\gamma \begin{bmatrix} \overset{e}{\mathbf{y}}_1 \\ \overset{e}{\mathbf{y}}_2 \\ \overset{e}{\mathbf{y}}_3 \end{bmatrix}, \quad (34)$$

in which $[\mathbf{N}(\gamma)] = [\mathbf{N}_1(\gamma) \mid \mathbf{N}_2(\gamma) \mid \mathbf{N}_3(\gamma)]$ is the number of elements (subintervals). Using Eq. (34) as a point of departure and repeating the line of thought leading to Eq. (31), once again we obtain an algebraic eigenvalue problem.

5. GREEN'S FUNCTION MATRICES FOR THE VIBRATIONS

5.1 Introductory remarks

Relying on the definition presented in Section 3, the calculation of Green's function matrices for loaded fixed-fixed beams is presented here. With regard to property (3) in the definition, the Green's function matrix can be given in the following form:

$$\underbrace{\mathbf{G}(\varphi,\psi)}_{(2\times 2)} = \sum_{j=1}^{4}\mathbf{Y}_j(\varphi)\left[\mathbf{A}_j(\psi) \pm \mathbf{B}_j(\psi)\right], \quad (35)$$

where: (a) the sign is [positive] (negative) if [$\varphi \geq \psi$] ($\varphi \leq \psi$); (b) the matrices $\mathbf{A}_j$ and $\mathbf{B}_j$ have the following structure:

$$\mathbf{A}_j = \begin{bmatrix} \overset{j}{A}_{11} & \overset{j}{A}_{12} \\ \overset{j}{A}_{21} & \overset{j}{A}_{22} \end{bmatrix} = \begin{bmatrix} \mathbf{A}_{j1} & \mathbf{A}_{j2} \end{bmatrix},$$
$$\mathbf{B}_j = \begin{bmatrix} \overset{j}{B}_{11} & \overset{j}{B}_{12} \\ \overset{j}{B}_{21} & \overset{j}{B}_{22} \end{bmatrix} = \begin{bmatrix} \mathbf{B}_{j1} & \mathbf{B}_{j2} \end{bmatrix} \quad j = 1,...,4; \quad (36)$$

(c) the coefficients in matrix $\mathbf{B}_j$ are independent of the boundary conditions.

Since the matrices $\mathbf{Y}_3$ and $\mathbf{Y}_4$ are different for the two cases of loading, these have to be addresses individually.

5.2 Calculation of Green's function matrix when $m\varepsilon_{o\xi}<1$

For the sake of brevity, let us now introduce the following notational conventions:

$$a = \overset{1}{B}_{1i}, \quad b = \overset{2}{B}_{1i}, \quad c = \overset{3}{B}_{1i}, \quad d = \overset{3}{B}_{2i}, \quad e = \overset{4}{B}_{1i}, \quad f = \overset{4}{B}_{2i}. \quad (37)$$

We observe that $\overset{1}{B}_{21} = \overset{2}{B}_{21} = \overset{1}{B}_{22} = \overset{2}{B}_{22} = 0$, see Section 3. The equation systems for the unknowns *a*, ..., *f* can be set up by fulfilling the continuity and discontinuity conditions for Green's function matrix at $\varphi = \psi$, on the basis of equations (25) – see properties (1) and (2). If *i=1* we have:

$$\begin{bmatrix} \cos\psi & -\sin\psi & \cos(\chi\psi) & \mathcal{M}\psi & -\sin(\chi\psi) & 1 \\ \sin\psi & \cos\psi & \chi\sin(\chi\psi) & -1 & \chi\cos(\chi\psi) & 0 \\ -\sin\psi & -\cos\psi & -\chi\sin(\chi\psi) & \mathcal{M} & -\chi\cos(\chi\psi) & 0 \\ \cos\psi & -\sin\psi & \chi^2\cos(\chi\psi) & 0 & -\chi^2\sin(\chi\psi) & 0 \\ -\sin\psi & -\cos\psi & -\chi^3\sin(\chi\psi) & 0 & -\chi^3\cos(\chi\psi) & 0 \\ -\cos\psi & \sin\psi & -\chi^4\cos(\chi\psi) & 0 & \chi^4\sin(\chi\psi) & 0 \end{bmatrix} \begin{bmatrix} a \\ b \\ c \\ d \\ e \\ f \end{bmatrix} = \begin{bmatrix} 0 \\ 0 \\ \frac{1}{2m} \\ 0 \\ 0 \\ 0 \end{bmatrix}, \quad (38)$$

from which it follows that:

$$a=\overset{1}{B}_{11}=\frac{\chi^2}{\left(1-\chi^2\right)(1-\mathcal{M})m}\frac{\sin\psi}{2},\qquad b=\overset{2}{B}_{11}=\frac{\chi^2}{\left(1-\chi^2\right)(1-\mathcal{M})m}\frac{\cos\psi}{2},$$
$$c=\overset{3}{B}_{11}=-\frac{\chi^2}{\left(1-\chi^2\right)(1-\mathcal{M})m}\frac{\sin\chi\psi}{2\chi^3},\qquad d=\overset{3}{B}_{21}=-\frac{1}{2(1-\mathcal{M})m},\tag{39}$$
$$e=\overset{4}{B}_{11}=-\frac{1}{\chi\left(1-\chi^2\right)(1-\mathcal{M})m}\frac{\cos\chi\psi}{2},\qquad f=\overset{4}{B}_{21}=\frac{1}{2}\mathcal{M}\frac{\psi}{m(1-\mathcal{M})}.$$

If $i=2$ then:

$$\begin{bmatrix}\cos\psi & -\sin\psi & \cos(\chi\psi) & \mathcal{M}\psi & -\sin(\chi\psi) & 1\\ \sin\psi & \cos\psi & \chi\sin(\chi\psi) & -1 & \chi\cos(\chi\psi) & 0\\ -\sin\psi & -\cos\psi & -\chi\sin(\chi\psi) & \mathcal{M} & -\chi\cos(\chi\psi) & 0\\ \cos\psi & -\sin\psi & \chi^2\cos(\chi\psi) & 0 & -\chi^2\sin(\chi\psi) & 0\\ -\sin\psi & -\cos\psi & -\chi^3\sin(\chi\psi) & 0 & -\chi^3\cos(\chi\psi) & 0\\ -\cos\psi & \sin\psi & -\chi^4\cos(\chi\psi) & 0 & \chi^4\sin(\chi\psi) & 0\end{bmatrix}\begin{bmatrix}a\\ b\\ c\\ d\\ e\\ f\end{bmatrix}=\begin{bmatrix}0\\ 0\\ 0\\ 0\\ 0\\ -\frac{1}{2}\end{bmatrix}\tag{40}$$

is the equation system and the solutions are:

$$a=\overset{1}{B}_{12}=\frac{1}{2}\frac{\cos\psi}{\left(1-\chi^2\right)},\qquad b=\overset{2}{B}_{12}=-\frac{1}{2}\frac{\sin\psi}{\left(1-\chi^2\right)},\qquad c=\overset{3}{B}_{12}=-\frac{1}{2}\frac{\cos\chi\psi}{\left(1-\chi^2\right)\chi^2},$$
$$d=\overset{3}{B}_{22}=0,\qquad e=\overset{4}{B}_{12}=\frac{1}{2}\frac{\sin\chi\psi}{\left(1-\chi^2\right)\chi^2},\qquad f=\overset{4}{B}_{22}=\frac{1}{2\chi^2}.\tag{41}$$

As regards the matrices $\mathbf{A}_j$, or which is the same, the unknown scalars:

$$\overset{1}{A}_{1i}(\psi),\quad \overset{2}{A}_{1i}(\psi),\quad \overset{3}{A}_{1i}(\psi),\quad \overset{3}{A}_{2i}(\psi),\quad \overset{4}{A}_{1i}(\psi),\quad \overset{4}{A}_{2i}(\psi)\qquad i=1,2;\qquad \psi\in[-\vartheta,\vartheta]$$

($\overset{1}{A}_{21}=\overset{2}{A}_{21}=\overset{1}{A}_{22}=\overset{2}{A}_{22}=0$), property (4) in Section 3, and boundary conditions given by Eq. (20b) yield the following system:

$$\begin{bmatrix}\cos\vartheta & \sin\vartheta & \cos(\chi\vartheta) & -\mathcal{M}\vartheta & \sin(\chi\vartheta) & 1\\ \cos\vartheta & -\sin\vartheta & \cos(\chi\vartheta) & \mathcal{M}\vartheta & -\sin(\chi\vartheta) & 1\\ -\sin\vartheta & \cos\vartheta & -\chi\sin(\chi\vartheta) & -1 & \chi\cos(\chi\vartheta) & 0\\ \sin\vartheta & \cos\vartheta & \chi\sin(\chi\vartheta) & -1 & \chi\cos(\chi\vartheta) & 0\\ \cos\vartheta & \sin\vartheta & \chi^2\cos(\chi\vartheta) & 0 & \chi^2\sin(\chi\vartheta) & 0\\ \cos\vartheta & -\sin\vartheta & \chi^2\cos(\chi\vartheta) & 0 & -\chi^2\sin(\chi\vartheta) & 0\end{bmatrix}\begin{bmatrix}\overset{1}{A}_{1i}\\ \overset{2}{A}_{1i}\\ \overset{3}{A}_{1i}\\ \overset{3}{A}_{2i}\\ \overset{4}{A}_{1i}\\ \overset{4}{A}_{2i}\end{bmatrix}=$$
$$=\begin{bmatrix}-a\cos\vartheta-b\sin\vartheta-c\cos(\chi\vartheta)+d\mathcal{M}\vartheta-e\sin(\chi\vartheta)-f\\ a\cos\vartheta-b\sin\vartheta+c\cos(\chi\vartheta)+d\mathcal{M}\vartheta-e\sin(\chi\vartheta)+f\\ a\sin\vartheta-b\cos\vartheta+c\chi\sin(\chi\vartheta)+d-e\chi\cos(\chi\vartheta)\\ a\sin\vartheta+b\cos\vartheta+c\chi\sin(\chi\vartheta)-d+e\chi\cos(\chi\vartheta)\\ -a\cos\vartheta-b\sin\vartheta-c\chi^2\cos(\chi\vartheta)-e\chi^2\sin(\chi\vartheta)\\ a\cos\vartheta-b\sin\vartheta+c\chi^2\cos(\chi\vartheta)-e\chi^2\sin(\chi\vartheta)\end{bmatrix}.\tag{42}$$

Let us introduce the constants:

$$C_{21} = \left(1-\chi^2\right)\sin\vartheta\sin\chi\vartheta + \mathcal{M}\chi\vartheta\left(\chi\cos\vartheta\sin\chi\vartheta - \sin\vartheta\cos\chi\vartheta\right),$$
$$D_{21} = \chi\sin\vartheta\cos\chi\vartheta - \cos\vartheta\sin\chi\vartheta \tag{43}$$

with which we can manipulate the solutions to Eq. (42) into these forms:

$$\overset{1}{A}_{1i} = \frac{1}{D_{21}}\left[b\left(\sin\vartheta\sin\chi\vartheta + \chi\cos\vartheta\cos\chi\vartheta\right) - d\chi\cos\chi\vartheta + e\chi^2\right],$$
$$\overset{2}{A}_{1i} = \frac{1}{C_{21}}\left(a\mathcal{M}\chi\vartheta\left(\chi\sin\vartheta\sin\chi\vartheta + \cos\vartheta\cos\chi\vartheta\right) - a\left(1-\chi^2\right)\cos\vartheta\sin\chi\vartheta + c\mathcal{M}\vartheta\chi^3 + f\chi^2\sin\chi\vartheta\right),$$
$$\overset{3}{A}_{1i} = -\frac{1}{D_{21}\chi}\left[b + e\chi\left(\chi\sin\vartheta\sin\chi\vartheta + \cos\vartheta\cos\chi\vartheta\right) - d\cos\vartheta\right],$$
$$\overset{3}{A}_{2i} = -\frac{1}{C_{21}}\left[a\left(1-\chi^2\right)\sin\chi\vartheta + c\chi\left(1-\chi^2\right)\sin\vartheta - f\chi\left(\chi\cos\vartheta\sin\chi\vartheta - \sin\vartheta\cos\chi\vartheta\right)\right],$$
$$\overset{4}{A}_{1i} = -\frac{1}{C_{21}}\left[a\mathcal{M}\vartheta + c\mathcal{M}\chi\vartheta\left(\chi\cos\vartheta\cos\chi\vartheta + \sin\vartheta\sin\chi\vartheta\right) + c\left(1-\chi^2\right)\sin\vartheta\cos\chi\vartheta + f\sin\vartheta\right],$$
$$\overset{4}{A}_{2i} = \frac{1}{D_{21}\chi}\left[b\left(1-\chi^2\right)\cos\chi\vartheta + d\mathcal{M}\chi\vartheta\left(\chi\sin\vartheta\cos\chi\vartheta - \cos\vartheta\sin\chi\vartheta\right) - \right.$$
$$\left. -d\left(1-\chi^2\right)\cos\vartheta\cos\chi\vartheta + e\chi\left(1-\chi^2\right)\cos\vartheta\right]. \tag{44}$$

5.3 Calculation of Green's function matrix if $m\varepsilon_{o\xi} > 1$

As regards $\overset{1}{B}_{1i},\ldots,\overset{4}{B}_{2i}$, on the basis of Eq. (38), it is not too difficult to verify that for $i=1$ the following equations should be solved:

$$\begin{bmatrix} \cos\psi & -\sin\psi & \cosh(\chi\psi) & \mathcal{M}\psi & \sinh(\chi\psi) & 1 \\ \sin\psi & \cos\psi & -\chi\sinh(\chi\psi) & -1 & -\chi\cosh(\chi\psi) & 0 \\ -\sin\psi & -\cos\psi & \chi\sinh(\chi\psi) & \mathcal{M} & \chi\cosh(\chi\psi) & 0 \\ \cos\psi & -\sin\psi & -\chi^2\cosh(\chi\psi) & 0 & -\chi^2\sinh(\chi\psi) & 0 \\ -\sin\psi & -\cos\psi & -\chi^3\sinh(\chi\psi) & 0 & -\chi^3\cosh(\chi\psi) & 0 \\ -\cos\psi & \sin\psi & -\chi^4\cosh(\chi\psi) & 0 & -\chi^4\sinh(\chi\psi) & 0 \end{bmatrix} \begin{bmatrix} a \\ b \\ c \\ d \\ e \\ f \end{bmatrix} = \begin{bmatrix} 0 \\ 0 \\ \frac{1}{2m} \\ 0 \\ 0 \\ 0 \end{bmatrix}, \tag{45}$$

for which:

$$a = \overset{1}{B}_{11} = -\frac{\chi^2}{\left(1+\chi^2\right)(1-\mathcal{M})m}\frac{\sin\psi}{2}, \quad b = \overset{2}{B}_{11} = -\frac{\chi^2}{\left(1+\chi^2\right)(1-\mathcal{M})m}\frac{\cos\psi}{2},$$
$$c = \overset{3}{B}_{11} = -\frac{1}{\chi\left(1+\chi^2\right)(1-\mathcal{M})m}\frac{\sinh\chi\psi}{2}, \quad d = \overset{3}{B}_{21} = -\frac{1}{2(1-\mathcal{M})m}, \tag{46}$$
$$e = \overset{4}{B}_{11} = \frac{1}{\chi\left(1+\chi^2\right)(1-\mathcal{M})m}\frac{\cosh\chi\psi}{2}, \quad f = \overset{4}{B}_{21} = \frac{1}{2(1-\mathcal{M})m}\mathcal{M}\psi$$

are the solutions. If $i=2$:

$$\begin{bmatrix} \cos\psi & -\sin\psi & \cosh(\chi\psi) & \mathcal{M}\psi & \sinh(\chi\psi) & 1 \\ \sin\psi & \cos\psi & -\chi\sinh(\chi\psi) & -1 & -\chi\cosh(\chi\psi) & 0 \\ -\sin\psi & -\cos\psi & \chi\sinh(\chi\psi) & \mathcal{M} & \chi\cosh(\chi\psi) & 0 \\ \cos\psi & -\sin\psi & -\chi^2\cosh(\chi\psi) & 0 & -\chi^2\sinh(\chi\psi) & 0 \\ -\sin\psi & -\cos\psi & -\chi^3\sinh(\chi\psi) & 0 & -\chi^3\cosh(\chi\psi) & 0 \\ -\cos\psi & \sin\psi & -\chi^4\cosh(\chi\psi) & 0 & -\chi^4\sinh(\chi\psi) & 0 \end{bmatrix} \begin{bmatrix} a \\ b \\ c \\ d \\ e \\ f \end{bmatrix} = \begin{bmatrix} 0 \\ 0 \\ 0 \\ 0 \\ 0 \\ -\frac{1}{2} \end{bmatrix} \tag{47}$$

is the equation system - compare it to Eq. (40) - and the solutions are as follows:

$$\begin{aligned} &a = \overset{1}{B}_{12} = \frac{1}{2}\frac{\cos\psi}{\left(1+\chi^2\right)}, \quad b = \overset{2}{B}_{12} = -\frac{1}{2}\frac{\sin\psi}{\left(1+\chi^2\right)}, \quad c = \overset{3}{B}_{12} = \frac{1}{2}\frac{\cosh\chi\psi}{\left(1+\chi^2\right)\chi^2}, \\ &d = \overset{3}{B}_{22} = 0, \quad e = \overset{4}{B}_{12} = -\frac{1}{2}\frac{\sinh\chi\psi}{\chi^2\left(1+\chi^2\right)}, \quad f = \overset{4}{B}_{22} = -\frac{1}{2\chi^2}. \end{aligned} \tag{48}$$

For the matrices $\mathbf{A}_j$, boundary conditions given by Eq. (20b) yield the equation system upon repeating the steps leading to Eq. (42), consequently:

$$\begin{bmatrix} \cos\vartheta & \sin\vartheta & \cosh(\chi\vartheta) & -\mathcal{M}\vartheta & -\sinh(\chi\vartheta) & 1 \\ \cos\vartheta & -\sin\vartheta & \cosh(\chi\vartheta) & \mathcal{M}\vartheta & \sinh(\chi\vartheta) & 1 \\ -\sin\vartheta & \cos\vartheta & \chi\sinh(\chi\vartheta) & -1 & -\chi\cosh(\chi\vartheta) & 0 \\ \sin\vartheta & \cos\vartheta & -\chi\sinh(\chi\vartheta) & -1 & -\chi\cosh(\chi\vartheta) & 0 \\ \cos\vartheta & \sin\vartheta & -\chi^2\cosh(\chi\vartheta) & 0 & \chi^2\sinh(\chi\vartheta) & 0 \\ \cos\vartheta & -\sin\vartheta & -\chi^2\cosh(\chi\vartheta) & 0 & -\chi^2\sinh(\chi\vartheta) & 0 \end{bmatrix} \begin{bmatrix} \overset{1}{A}_{1i} \\ \overset{2}{A}_{1i} \\ \overset{3}{A}_{1i} \\ \overset{3}{A}_{2i} \\ \overset{4}{A}_{1i} \\ \overset{4}{A}_{2i} \end{bmatrix} =$$

$$= \begin{bmatrix} -a\cos\vartheta - b\sin\vartheta - c\cosh(\chi\vartheta) + d\mathcal{M}\vartheta + e\sinh(\chi\vartheta) - f \\ a\cos\vartheta - b\sin\vartheta + c\cosh(\chi\vartheta) + d\mathcal{M}\vartheta + e\sinh(\chi\vartheta) + f \\ a\sin\vartheta - b\cos\vartheta - c\chi\sinh(\chi\vartheta) + d + e\chi\cosh(\chi\vartheta) \\ a\sin\vartheta + b\cos\vartheta - c\chi\sinh(\chi\vartheta) - d - e\chi\cosh(\chi\vartheta) \\ -a\cos\vartheta - b\sin\vartheta + c\chi^2\cosh(\chi\vartheta) - e\chi^2\sinh(\chi\vartheta) \\ a\cos\vartheta - b\sin\vartheta - c\chi^2\cosh(\chi\vartheta) - e\chi^2\sinh(\chi\vartheta) \end{bmatrix}, \tag{49}$$

from where, with the constants:

$$\begin{aligned} &\mathcal{C}_{21} = -\left(1+\chi^2\right)\sin\vartheta\sinh\chi\vartheta + \chi\mathcal{M}\vartheta\left(\chi\cos\vartheta\sinh\chi\vartheta + \sin\vartheta\cosh\chi\vartheta\right), \\ &\mathcal{D}_{21} = \chi\sin\vartheta\cosh\chi\vartheta - \cos\vartheta\sinh\chi\vartheta \end{aligned}, \tag{50}$$

the closed form solutions are:

$$
\begin{aligned}
&{}^{1}A_{1i} = \frac{1}{\mathcal{D}_{21}}\Big(b\big(\sin\vartheta\sinh\chi\vartheta + \chi\cos\vartheta\cosh\chi\vartheta\big) - d\,\chi\cosh\chi\vartheta - \chi^2 e\Big),\\
&{}^{2}A_{1i} = \frac{a\mathcal{M}\vartheta\chi\big(\chi\sin\vartheta\sinh\chi\vartheta - \cos\vartheta\cosh\chi\vartheta\big) + a\big(1+\chi^2\big)\cos\vartheta\sinh\chi\vartheta + c\mathcal{M}\vartheta\chi^3 + f\chi^2\sinh\chi\vartheta}{\mathcal{C}_{21}},\\
&{}^{3}A_{1i} = \frac{1}{\mathcal{D}_{21}\chi}\Big[b + e\chi\big(\chi\sin\vartheta\sinh\chi\vartheta - \cos\vartheta\cosh\chi\vartheta\big) - d\cos\vartheta\Big],\\
&{}^{3}A_{2i} = \frac{1}{\mathcal{C}_{21}}\Big[a\big(1+\chi^2\big)\sinh\chi\vartheta + c\chi\big(1+\chi^2\big)\sin\vartheta + f\chi\big(\chi\cos\vartheta\sin\chi\vartheta + \sin\vartheta\cos\chi\vartheta\big)\Big],\\
&{}^{4}A_{1i} = -\frac{1}{\mathcal{C}_{21}}\Big[a\mathcal{M}\vartheta - c\mathcal{M}\vartheta\chi\big(\chi\cos\vartheta\cosh\chi\vartheta + \sin\vartheta\sinh\chi\vartheta\big) + c\big(1+\chi^2\big)\sin\vartheta\cosh\chi\vartheta + f\sin\vartheta\Big],\\
&{}^{4}A_{2i} = \frac{1}{\mathcal{D}_{21}\chi}\Big(-b\big(1+\chi^2\big)\cosh\chi\vartheta + d\mathcal{M}\chi\vartheta\big(\chi\sin\vartheta\cosh\chi\vartheta - \cos\vartheta\sinh\chi\vartheta\big) +\\
&\qquad + d\big(1+\chi^2\big)\cos\vartheta\cosh\chi\vartheta + e\chi\big(1+\chi^2\big)\cos\vartheta\Big). \qquad (51)
\end{aligned}
$$

6. THE LOAD-STRAIN RELATIONSHIP AND THE CRITICAL STRAIN

6.1 Load-strain relationship

It is essential to know how the load affects the strain of the centroidal axis. In practice, load is always the known quantity. However, our formulation has the axial strain $\varepsilon_{o\xi}$ as parameter. As the model is linear, the effects the deformations have on the equilibrium state are negligible. We can establish the relationship $\varepsilon_{o\xi} = \varepsilon_{o\xi}(\mathcal{P})$ on the basis of differential equations (9), which are to be solved by assuming $f_t = f_n = 0$. For a fixed-fixed beam, differential equations (9) are associated with the boundary conditions:

$$U_o\big|_{\pm\vartheta} = W_o\big|_{\pm\vartheta} = \psi_{o\eta}\big|_{\pm\vartheta} = 0 \qquad (52a)$$

and the continuity (discontinuity) conditions:

$$
\begin{aligned}
&U_o\big|_{\varphi=-0} = U_o\big|_{\varphi=+0}, \qquad W_o\big|_{\varphi=-0} = W_o\big|_{\varphi=+0},\\
&\psi_{o\eta}\big|_{\varphi=-0} = \psi_{o\eta}\big|_{\varphi=+0},
\end{aligned} \qquad (52b)
$$

$$
\begin{aligned}
&N\big|_{\varphi=-0} = N\big|_{\varphi=+0}, \qquad M\big|_{\varphi=-0} = M\big|_{\varphi=+0},\\
&\left.\frac{dM}{ds}\right|_{\varphi=+0} - \left.\frac{dM}{ds}\right|_{\varphi=-0} - P_\zeta = 0
\end{aligned} \qquad (52c)
$$

prescribed at the crown point. Here, the axial strain $\varepsilon_{o\xi}$, the angle of rotation $\psi_{o\eta}$, the axial force N as well as the bending moment M can all be expressed with the dimensionless displacements U_o and W_o (more details are presented in the M.Sc. Thesis [15]:

$$\varepsilon_{o\xi} = U_o^{(1)} + W_o, \quad \psi_{o\eta} = U_o - W_o^{(1)} \qquad (53a)$$

$$N = A_e\varepsilon_{o\xi} - \frac{M}{\rho_o} \approx A_e\varepsilon_{o\xi}, \qquad (53b)$$

$$M = -\frac{I_{e\eta}}{\rho_o^2}\Big(W_o^{(2)} + W_o\Big). \qquad (53c)$$

The long formal transformations lead to the axial strain as:

$$\varepsilon_{o\xi} = \frac{\mathcal{P}}{\vartheta}\frac{-\big(1-\cos\vartheta\big)\big(\sin\vartheta - \vartheta\big)}{\vartheta\big(1+m\big)\big[\vartheta + \sin\vartheta\cos\vartheta\big] - 2m\sin^2\vartheta}. \qquad (54)$$

If $\mathcal{P}$ is [negative] (positive), then $\varepsilon_{0\xi}$ is [negative] (positive).

6.2 The critical strain

When reaching the critical strain, the heterogeneous curved beam in compression loses its stability. This limit can be obtained by solving the eigenvalue problems defined by Eqs. (15) with the right side set to zero (the beam is in a static equilibrium under the force exerted at the crown point) and by the corresponding homogeneous boundary conditions. In this case, physically, the lowest possible value of χ is sought.

The general solutions for the displacement increments are:

$$
\begin{aligned}
W_{ob} = &-E_2 - E_3\cos\varphi + E_4\sin\varphi -\\
&-\chi E_5\cos\chi\varphi + \chi E_6\sin\chi\varphi,
\end{aligned} \qquad (55a)
$$

$$
\begin{aligned}
U_{ob} = &E_1 + E_2\mathcal{M}\varphi + E_3\sin\varphi + E_4\cos\varphi +\\
&+E_5\sin\chi\varphi + E_6\cos\chi\varphi
\end{aligned} \qquad (55b)
$$

in which E_i $(i = 1, ..., 6)$ are undetermined constants of integration. For a fixed-fixed beam:

$$U_{ob}\big|_{\pm\vartheta} = W_{ob}\big|_{\pm\vartheta} = W_{ob}^{(1)}\Big|_{\pm\vartheta} = 0 \qquad (56)$$

are the boundary conditions. Therefore, the system of equations to be dealt with is:

$$\begin{bmatrix} 0 & 1 & \cos\vartheta & -\sin\vartheta & \chi\cos\chi\vartheta & -\chi\sin\chi\vartheta \\ 0 & 1 & \cos\vartheta & \sin\vartheta & \chi\cos\chi\vartheta & \chi\sin\chi\vartheta \\ 0 & 0 & \sin\vartheta & \cos\vartheta & \chi^2\sin\chi\vartheta & \chi^2\cos\chi\vartheta \\ 0 & 0 & -\sin\vartheta & \cos\vartheta & -\chi^2\sin\chi\vartheta & \chi^2\cos\chi\vartheta \\ 1 & \mathcal{M}\vartheta & \sin\vartheta & \cos\vartheta & \sin\chi\vartheta & \cos\chi\vartheta \\ 1 & -\mathcal{M}\vartheta & -\sin\vartheta & \cos\vartheta & -\sin\chi\vartheta & \cos\chi\vartheta \end{bmatrix} \begin{bmatrix} E_1 \\ E_2 \\ E_3 \\ E_4 \\ E_5 \\ E_6 \end{bmatrix} = \begin{bmatrix} 0 \\ 0 \\ 0 \\ 0 \\ 0 \\ 0 \end{bmatrix}. \tag{57}$$

Nontrivial solution can be obtained if we set the determinant of the coefficient matrix to zero, thus:

$$D = -8\chi\left(-\cos\vartheta\sin\chi\vartheta + \chi\sin\vartheta\cos\chi\vartheta\right)\times$$
$$\times\left(-\chi^2\sin\vartheta\sin\chi\vartheta + \chi^2\mathcal{M}\vartheta\cos\vartheta\sin\chi\vartheta - \mathcal{M}\vartheta\left(\sin\vartheta\cos\chi\vartheta\right)\chi + \sin\vartheta\sin\chi\vartheta\right) = 0. \tag{58}$$

In this way there are three solutions:

$$\chi = 0, \qquad \chi\sin\vartheta\cos\chi\vartheta = \cos\vartheta\sin\chi\vartheta, \tag{59}$$

$$\sin\chi\vartheta\left(\chi^2\mathcal{M}\vartheta\cos\vartheta + \sin\vartheta\right) = \sin\vartheta\left(\mathcal{M}\vartheta\chi\cos\chi\vartheta + \chi^2\sin\chi\vartheta\right) \tag{60}$$

from which, physically, the lowest possible one is obtained from the second equation in Eqs. (59):

$$\chi\tan\vartheta = \tan\chi\vartheta\,. \tag{61}$$

The approximative polynomial that satisfies the above relation with a very good accuracy is:

$$\chi\vartheta = g_{ff}\left(\vartheta\right) = 3.689\,334\,516\times10^{-2}\vartheta^4 - 0.131\,139\,9068\vartheta^3 + 0.259\,573\,7664\vartheta^2 -$$
$$-9.600\,584\,516\times10^{-2}\vartheta + 4.506\,225\,066\,. \tag{62}$$

It means that the critical strain calculated from Eq. (21) is:

$$\varepsilon_{o\xi\,crit} = -\frac{1}{m}\left[\left(\frac{g_{ff}}{\vartheta}\right)^2 - 1\right]. \tag{63}$$

7. COMPUTATIONAL AND EXPERIMENTAL RESULTS

A program has been developed in Fortran90 to numerically solve the eigenvalue problems governed by the Fredholm integral equations. The results have been compared to those valid for the free vibrations of curved beams with the same geometric and material properties. (For a more detailed study about the natural frequencies of planar curved beams see Ref. [5].

7.1 Numerical results for free vibrations

When we set the strain, and at the same time the parameter χ to a very small magnitude – i.e. $|\varepsilon_{o\xi}| = |\varepsilon_{o\xi\,crit}\cdot10^{-6}|$ – for both loading cases we get back identical results obtained in Refs. [5] and [16] for the free vibrations.

It is known, see Ref. [13], that the *i*-th eigenfrequency for the free transverse vibrations of heterogeneous straight beams can be calculated from the relation:

$$\alpha_i^* = \frac{C_{i,char}\pi^2}{\sqrt{\frac{\rho_a A}{I_{e\eta}}\ell_b^4}}. \tag{64}$$

Here, the constant $C_{i,char}$ depends on the supports and the number of the frequency sought (see Table 1), while l_b is the length of the beam.

If we recall Eq. $(16)_2$ which, for such a small strain considered, expresses the relation between the eigenvalues λ_i and the eigenfrequencies $\alpha_i = \alpha_{i\,free}$ for the free vibrations of curved beams, we arrive at relation:

$$C_{i,char}\frac{\alpha_i}{\alpha_i^*} = \frac{\sqrt{\lambda_i}}{\frac{\pi^2}{\sqrt{\frac{\rho_a A}{I_{e\eta}}\ell_r^2}}} = \frac{\overline{\vartheta}^2\sqrt{\lambda_i}}{\pi^2}. \tag{65}$$

This, therefore, expresses the relation between the natural frequencies of curved and straight beams with the same length ($\ell_b = R\overline{\vartheta}$) and same material. In Figure 2 the above ratio is plotted against the central angle $\overline{\vartheta}$ of the curved beam. Four different values of the parameter *m* were picked: *1000*; *3400*; *12000* and *100000*.

Table 1 The values of $C_{i,char}$

Support type	$i=1$	$i=2$	$i=3$	$i=4$
Fixed-fixed beam	*2.266*	*6.243*	*12.23*	*20.25*

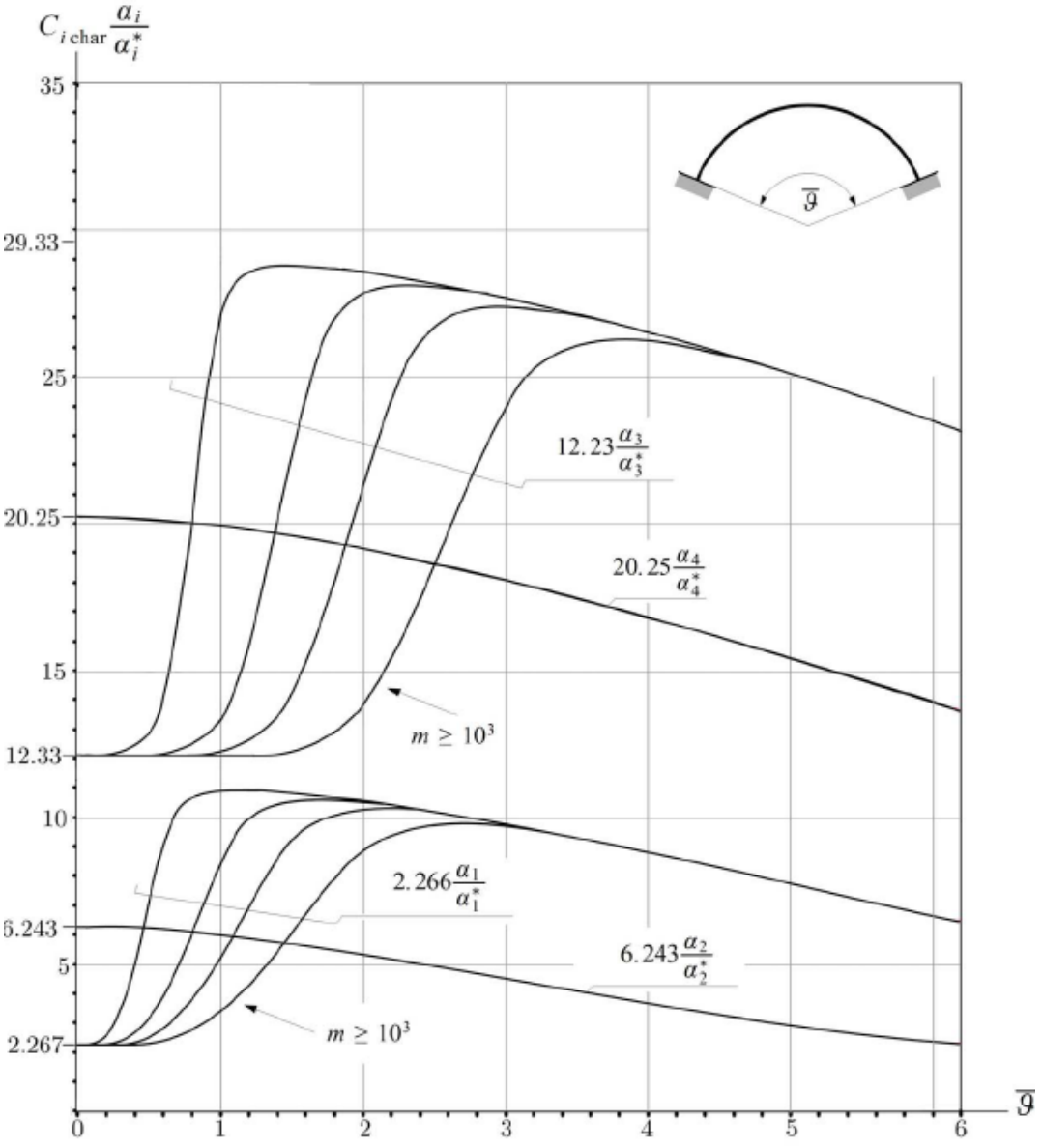

Fig. 2 Results for fixed-fixed beams when $\varepsilon_{o\xi} \cong 0$

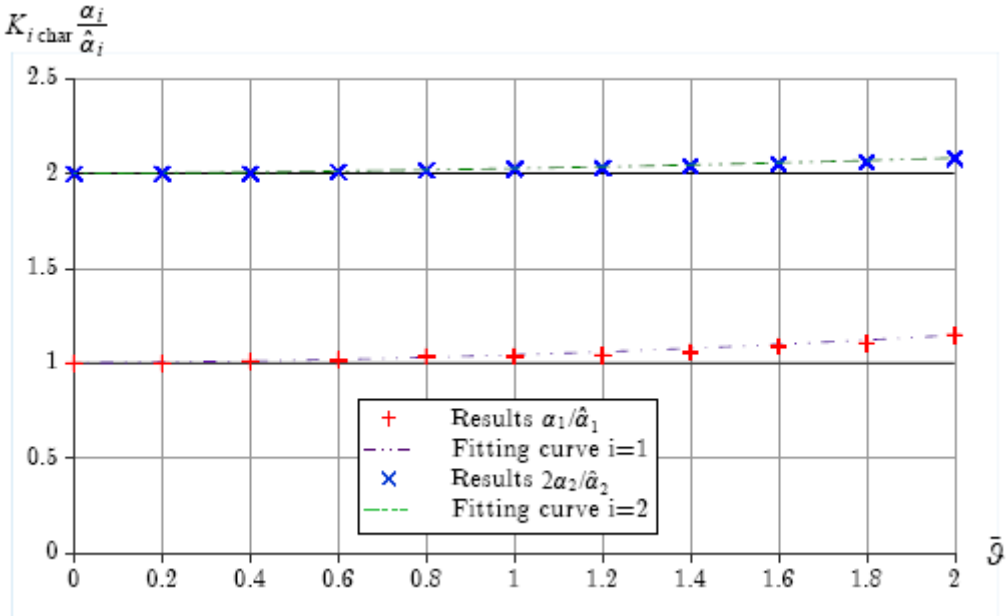

Fig. 3 A comparison with vibrating rods when $\varepsilon_{o\xi} \cong 0$

Observe that the ratio of the even natural frequencies are independent of *m*, while the odd ones depend enormously on it if the central angle is rather small. It is also important to mention that the frequency spectrum changes as $\overline{\vartheta}$ increases, e.g. the first/third eigenfrequency becomes the second/fourth one in terms of magnitude if $\overline{\vartheta}$ is sufficiently big.

Relying on Ref. [16], when dealing with the free longitudinal vibrations of fixed-fixed rods, the natural frequencies assume the following form:

$$\hat{\alpha}_i = \frac{K_{i\,char}}{\ell_r}\sqrt{\frac{E}{\rho_a}}\pi\,, \tag{66}$$

where the constant $K_{ichar} = 1$; ($i = 1, 2, 3, ...$) and l_r is the length of the rod.

If we recall Eq. $(16)_2$ again, we can compare this result with the free vibrations of curved beams $|\varepsilon_{o\xi}| = |\varepsilon_{o\ \xi crit}\cdot 10^{-6}| \cong 0$ (when calculating the eigenvalues λ_i) in such a way that:

$$K_{i\,char}\frac{\alpha_i}{\hat{\alpha}_i} = \frac{1}{\sqrt{m}}\frac{\overline{\vartheta}}{\pi}\sqrt{\lambda_i}\,. \tag{67}$$

These quotients for $i = 1, 2$ are plotted in Figure 3. It turns out that the ratios do not depend on the parameter *m* and are equal to *1* and *2*, respectively, if the central angle is small enough. It is also interesting to mention that, when the curved beam is pinned-pinned, there are hardly any noticeable differences. The equations of the fitting curves are:

$$\frac{\alpha_1}{\hat{\alpha}_1} = 1.001118\,881 + $$
$$+0.010\,891\,608\,\overline{\vartheta} + 0.031\,031\,468\,\overline{\vartheta}^2\,, \tag{68a}$$

$$2\frac{\alpha_2}{\hat{\alpha}_2} = 1.999\,126\,573 + $$
$$+0.012\,572\,027\,\overline{\vartheta} + 0.014\,195\,804\,\overline{\vartheta}^2\,. \tag{68b}$$

7.2 Experimental determination of the eigenfrequencies

Aiming to confirm the theoretical results, we began high-accuracy experimental investigations. A membrane-less VISATON EX 45S loudspeaker (with *10 W* output) was chosen as an excitatory device. It was fixed to the crown of the curved beam with a screw; to better understand the set-up, see Figure 4.

The total additional mass at the crown is $m = 74$ *g*, that is ~ *0,794 N*. The original electronic system – with signals generated by a free-to-access software SweepGen 3.5.2.24 (http://www.satsignal.eu) – can realize the desired output frequency range. The VISATON EX 45S electro-dynamical exciter is practically a membrane-less loudspeaker and its moving coil acts directly on the studied structural member.

A high-performance electronic amplifier circuit drives the exciter at the required voltage and power (AD-022 amplifier module, www.adelaida.ro). It is presented in Figure 5. This High-Fidelity amplifier module is based on a TDA7294 amplifier integrated circuit, which has utterly preferable technical parameters. The amplifier can output a maximum of *100 W* power, when using a *±38 V* supply, but for the experiments (in order to protect the exciter) the supply voltage was limited to *±22 V*. The power supply, presented in Figure 6, is a simple one, because the amplifier circuit has a very good differential supply voltage ripple rejection. It consists of a *230* V/*2×19 V*, *1A* mains transformer, a *3A* bridge rectifier and *2×4.7 mF* filtering electrolytic condensers. There is a *200 cm²* heat sink attached to the integrated power amplifier circuit.

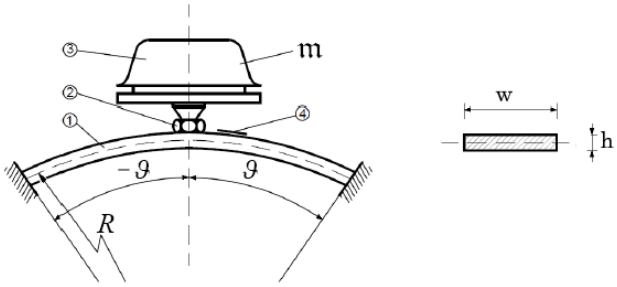

Fig. 4 The experimental set-up: (1) curved beam; (2) fixing screw of the (3) excitatory device; (4) strain gauge

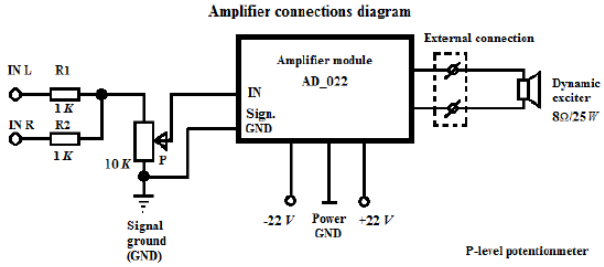

Fig. 5 The schematic of the amplifier connections

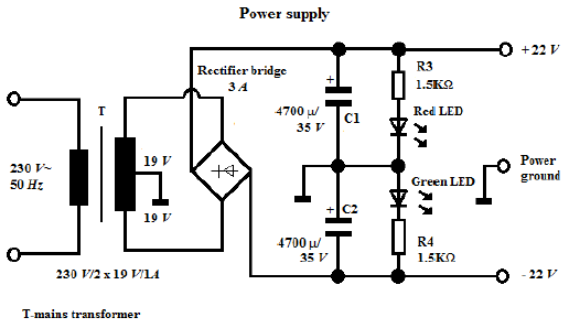

Fig. 6 The schematic of the power supply circuit

The input signal is generated by a computer software. There is a bunch of signal generator programmes available on the Internet. In our experiments, the free Sweep-Gen 3.5.2.24 has been used. This is a simple, but at the same time, very effective audio signal generator. It has a lot of presets, e.g. sine/square shape, separate *L*/*R* levels and frequencies, preset and custom frequency ranges,

various sweep modes and noise, etc. The input signal was sent from the *3.5 mm* stereo jack audio port of a computer. The input sensitivity was found to be sufficiently good. Both the left and right channels were used with *2×1 kΩ* resistors for protection and separation. A *10 kΩ* potentiometer made it possible to set the desired input level.

Each of the curved beams was equipped with an HBM simple-grid electric strain gauge – see part (4) in Figure 4. The active length of the strain gauge was *10 mm*, while the electric resistance was *120 Ω*. The strain gauge was connected to a quarter Wheatstone bridge to monitor the occuring strains due to the mechanical vibrations. During the experiments, the authors investigated a frequency range of *5 ... 2500* Hz, with a sampling rate of *20000/s*, using a multichannel National Instruments series *6000* data acquisition device. Two channels were involved: the first one for the excitation signal and the other one for receiving the signals from the strain gauges.

In an attempt to improve the accuracy of the received frequencies, the authors have used customized settings instead of the default ones under SweepGen 3.5.2.24. This new program counts how many times the signal passes through the zero value and, based on this information, we could determine the exact frequency of the exciter. Given the fact that the sample rate was *20000* per second, the obtained frequencies were more reliable and correctly determined. A very first attempt was made on a sweep frequency mode in the initially predicted *5 ... 2500 Hz* range. As a result, with a manual command, it became feasible to monitor the environment of the expected eigenfrequencies in order to find protuberant amplitudes of the signal coming from the strain gauge. A particular attention has been given to filtering out the eigenfrequencies of the exciter.

Due to the technical limits, we determined only the first (lowest) eigenfrequency of the four investigated beams. In the near future, the authors intend to study a larger range of eigenfrequencies with more sensitive devices.

The measured and in several ways computed first eigenfrequencies of the homogeneous curved beams ($E = 2.06 \cdot 10^5$ *MPa*, $\rho_a = 7800$ *kg/m*^{3}) are compared in Table 2, where the relative error was calculated by the following formula:

$$\Delta = \frac{\alpha_{1,Num} - \alpha_{1,Meas}}{\alpha_{1,Meas}} \cdot 100[\%] \,. \qquad (69)$$

Utilizing the commercial finite element software ABAQUS CAE 6.7., the additional mass at the crown was modelled by an increased density of the beam. Three-node B31 beam elements were used and the Linear Perturbation Frequency step. The outcomes are outlined by $\alpha_{1\ Abaqus}$ in the corresponding table.

The $\alpha_{1\ Ansys}$ outcomes of the software ANSYS were established by using 3D elements and a concentrated mass at the crown.

For the numerical model (based on the Green's function matrices), we replaced the additional mass m with a concentrated force of *0.794 N*. It was found that the strains caused by such a small force are in the magnitude of $(1.6 \cdot 10^{-4} \ ... \ 4.9 \cdot 10^{-5}) \cdot \varepsilon_{o\xi\ crit}$ and, therefore, have no effect on the frequencies. Consequently, we got back the results valid for free vibrations – see $\alpha_{1\ Num}$ in Table 2.

Between the numerical and experimental results, the difference is always less than *10%*. It is considered to be a good correlation.

Table 2. Results for the frequencies

m	2ϑ	$\omega \times h$	R	Beam weight	$\alpha_{1\ Abaqus}$	$\alpha_{1\ Num}$	$\alpha_{1\ Ansys}$	$\alpha_{1\ Meas}$	Δ
[-]	[°]	[mm^2]	[mm]	[N]	[Hz]	[Hz]	[Hz]	[Hz]	[%]
98 523	46	29.7 × 4.8	434.9	3.81	556.2	557.5	540.1	507	9.96
84 984	43.1	25 × 5.5	462.9	3.66	643.2	645.2	624.9	614	5.08
77 961	36.9	29.5 × 5	403	2.93	1057.8	1062.8	1028	1016	4.6
281 169	31.17	25.6 × 3.1	474.5	1.57	667.6	668.8	642.5	625	7

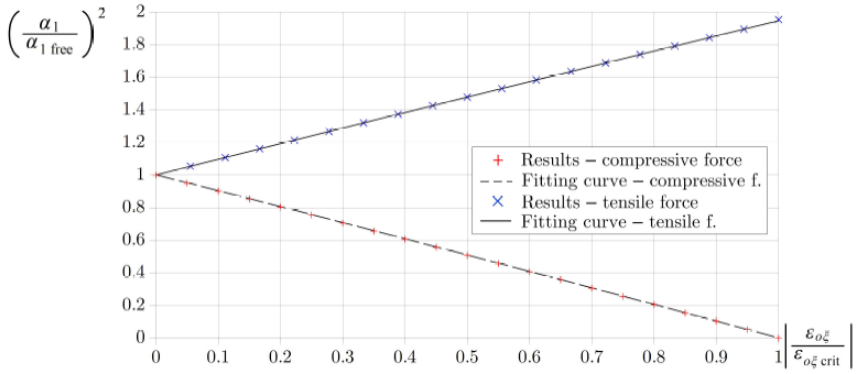

Fig. 7 Results for loaded curved beams

7.3 Results for beams under a concentrated force

The effect of the central concentrated load on the length of the centroidal axis is accounted for. In this subsection, α_i denotes the *i*-th eigenfrequency of the loaded beam, while the eigenfrequencies of the free vibrations (when the beam is unloaded) are noted by $\alpha_{i\ free}$. Figure 7 presents the quotient $\alpha_1^2 / \alpha_{1\,free}^2$ against the quotient $|\varepsilon_{o\xi} / \varepsilon_{o\xi\ crit}|$, when the loading is directed both, upwards and downwards. We point out that in this case the subscript *1* refers to the lowest frequency (which is not always the first one in the frequency numbering scheme that is shown in Figure 2). The ratios investigated are practically independent of *m* and ϑ. While for pinned-pinned beams, these ratios valid for [compression] <tension> [decrease] <increase> linearly, this time it is better to add a quadratic term to the approximative polynomials for a better accord. Equations:

$$\frac{\alpha_1^2}{\alpha_{1\ free}^2} = 1.00190 - 0.968\,24\frac{|\varepsilon_{o\xi}|}{\varepsilon_{o\xi\ crit}} - 0.032\,80\left(\frac{\varepsilon_{o\xi}}{\varepsilon_{o\xi\ crit}}\right)^2, \quad \text{if} \quad \varepsilon_{o\xi} < 0 \tag{70}$$

$$\frac{\alpha_1^2}{\alpha_{1\ free}^2} = 1.000\,904\,330 + 0.965\,029\,372\frac{|\varepsilon_{o\xi}|}{\varepsilon_{o\xi\ crit}} - 0.018\,791\,494\left(\frac{\varepsilon_{o\xi}}{\varepsilon_{o\xi\ crit}}\right)^2, \quad \text{if} \quad \varepsilon_{o\xi} > 0. \tag{71}$$

agree well with the computational results.

8. CONCLUDING REMARKS

We have investigated the vibrations of curved beams with cross-sectional heterogeneity and subjected to a vertical force at the crown point.

1) We have derived the governing equations of those boundary value problems which determine how the radial load affects the natural frequencies.
2) For a fixed-fixed beam, we have determined Green's function matrix assuming that the beam is prestressed by radial load. When computing this matrix we had to take into account that the system of ODEs that govern the problem are degenerated.
3) Making use of Green's function matrix we have reduced the self-adjoint eigenvalue problem set up for the eigenfrequencies to an eigenvalue problem governed by a homogeneous system of Fredholm integral equations. These integral equations can be used for those dead loads which result in a constant axial strain on the *E*-weighted centroidal axis (that is, for a constant radial load as well).
4) Numerical solutions were provided for fixed-fixed beams. The quotient $\alpha_1^2 / \alpha_{1\,free}^2$ depends almost linearly on the axial strain $\varepsilon_{o\xi}$ and is independent of the parameter *m*. Knowing the relationship $\varepsilon_{o\xi} = \varepsilon_{o\xi}(\mathcal{P})$, we can determine that value of $\varepsilon_{o\xi}$ which belongs to a given load and consequently the natural frequency of the loaded structure.
5) The numerical results were verified by commercial finite element calculations and experiments. It turns out that the numerical model approximates the eigenfrequencies with good accuracy.

9. ACKNOWLEDGEMENT BY THE FIRST AUTHOR

This research was supported by the **European Union** and the **State of Hungary**, **co-financed by the European Social Fund** in the framework of TÁMOP-4.2.4.A/2-11/1-2012-0001 'National Excellence Program'.

10. ACKNOWLEDGEMENTS

This paper was supported by the **Sectoral Operational Programme Human Resources Development** (SOP HRD), ID 134378 and ID 137070, financed from the **European Social Fund** and by the **Romanian Government**.

11. REFERENCES

[1] A.E.H. Love, *A Treatese on the Mathematical Theory of Elasticity*, Dower, New York, 1944.
[2] S. Markus and T. Nanasi, Vibration of curved beams, *The Shock and Vibration Digest*, Vol. 13, No. 4, pp. 3–14, 1981.
[3] P.A.A. Laura and M.J. Maurizi, Recent research on vibrations of arch-type structures, *The Shock and Vibration Digest*, Vol. 19, No. 1, pp. 6–9, 1987.
[4] P. Chidamparam and A.W. Leissa, Vibrations of planar curved beams, rings and arches, *ASME Applied Mechanics Reviews*, Vol. 46, No. 9, pp. 467–483, 1993.
[5] G. Szeidl, Effect of change in length on the natural frequencies and stability of circular beams, Ph.D. Thesis, Department of Mechanics, University of Miskolc, Miskolc, 1975. (in Hungarian)
[6] C.S. Huang, K.Y. Nieh and M.C. Yang, In-plane free vibration and stability of loaded and shear-deformable circular arches, *International Journal of Solids and Structures*, Vol. 40, No. 22, pp. 5865–5886, 2003.

[7] A. Yousefi and A. Rastgoo, Free vibration of functionally graded spatial curved beams, *Composite Structures*, Vol. 93, No. 11, pp. 3048–3056, 2011.
[8] M. Hajianmaleki and M.S. Qatu, Static and vibration analyses of thick, generally laminated deep curved beams with different boundary conditions, *Composites Part B: Engineering*, Vol. 43, No. 4, pp. 1767–1775, 2012.
[9] B. Kovács, Vibration analysis of layered curved arch, *Journal of Sound and Vibration*, Vol. 332, No. 18, pp. 4223–4240, 2013.
[10] F.F. Çalim, Forced vibration of curved beams on two-parameter elastic foundation, *Applied Mathematical Modelling*, Vol. 36, No. 3, pp. 964–973, 2012.
[11] R. Lawther, On the straightness of eigenvalue interactions, *Computational Mechanics*, Vol. 37, No. 4, pp. 362–368, 2005.
[12] G. Szeidl and L. Kiss, A nonlinear mechanical model for heterogeneous curved beams, Proc. of the 4th Int. Conf. on Advanced Composite Materials Engineering - COMAT2012, Brasov, Ed. M.M. Deidu, Derc Publishing House, Boston, pp. 31–39, 2012.
[13] L.P. Kiss, Free vibrations of heterogeneous curved beams, GEP Magazin, LXIV, No. 5, pp. 16–21, 2013. (in Hungarian)
[14] Ch.T.H. Baker, *The Numerical Treatment of Integral Equations*, Clarendon Press, Oxford, 1977.
[15] L. Kiss, Solutions to some problems of heterogeneous curved beams, M.Sc. Thesis, Department of Mechanics, University of Miskolc, Miskolc, 2011. (in Hungarian)
[16] G. Szeidl, K. Kelemen and A. Szeidl, Natural frequencies of a circular arch – Computations by the use of Green functions, *Publications of the University of Miskolc, Series D, Natural Sciences, Mathematics*, Vol. 38, No. 1, pp. 117–132, 1998.

VIBRACIJE OBOSTRANO UKLJEŠTENIH, HETEROGENIH ZAKRIVLJENIH GREDNIH NOSAČA OPTEREĆENIH CENTRIČNOM SILOM U NAJVIŠOJ TOČCI

SAŽETAK

U radu je prikazana analiza vibracija heterogenih zakrivljenih grednih nosača izloženih djelovanju opterećenja vlastitom težinom koja djeluje okomito na os nosača. Analiza je provedena uz pretpostavku (a) konstantnog radijusa zakrivljenosti, (b) ovisnosti Youngova modula elastičnosti i Poissonova koeficijenta o koordinatama poprečnog presjeka. Za slučaj obostrano uklještenih zakrivljenih grednih nosača, ciljevi ovoga rada su sljedeći: (1) odrediti matricu Greenove funkcije uz uvjet da je gredni nosač izložen opterećenju u radijalnom smjeru; (2) analizirati utjecaj opterećenja na promjenu vlastite frekvencije u slučaju kad je gredni nosač izložen vertikalnoj sili u svojoj najvišoj točci; (3) razviti numerički model koji bi omogućio određivanje međusobnog utjecaja vlastitih frekvencija i opterećenja. Rezultati numeričkog modeliranja prikazani su u grafičkom obliku.

Ključne riječi: *zakrivljeni gredni nosač, heterogeni materijal, vlastita frekvencija kao funkcija ovisn o opterećenju, matrica Greenove funkcije.*